Monitoring Steel Bridges by Acoustic Emission

AL GHORBANPOOR

The acoustic emission (AE) technique was used to locate fatigue crack initiation sites and to characterize signals related to fatigue cracks in bridge structural components. An experimental study that included a series of tests on welded and rolled beams was performed. Time and frequency domain analyses were performed on AE signals obtained during various life stages of each specimen. The effect on the AE signals of welding, which changed the material's microstructure, was studied. Two stress ranges and their effect on the AE signals were investigated. An in-service bridge was tested to study its general AE response. AE signals from growing fatigue cracks had distinct characteristics in both the time and frequency domains. Growing fatigue cracks were detected at relatively early stages of the fatigue lives and the corresponding AE signals were characterized throughout the experiments.

Fatigue crack behavior in structural steel components of highway bridges has been studied extensively through detailed theoretical and experimental investigations (*1–3*). The concept of fracture mechanics is used to evaluate fracture behavior and to predict the remaining fatigue lives of the structural members that contain cracks.

Using the fracture mechanics approach, the stress state adjacent to the tip of an existing crack, which is described by the stress intensity factor K, is normally examined. For example, the value of K for an infinite plate with a centrally located through-crack of size $2a$ and subjected to a remotely applied and uniformly distributed stress σ may be expressed as

$$K = \sigma(\pi a)^{1/2} \tag{1}$$

In general, Equation 1 can be written as

$$K = Y\sigma(\pi a)^{1/2} \tag{2}$$

where Y, a correction factor, is a function of the geometry of the crack and the cracked element under study.

The rate of crack growth per cycle (da/dN) increases exponentially with increased crack length (*4*), and is written as

$$\frac{da}{dN} = C(K_{max} - K_{min})^n \tag{3}$$

where C is the da/dN axis intercept in the da/dN versus fatigue life graph, and n is the slope of the crack growth rate curve.

Department of Civil Engineering and Mechanics, University of Wisconsin at Milwaukee, P.O. Box 784, Milwaukee, Wis. 53201.

Both C and n are material constants, and K_{max} and K_{min} are the stress intensity factors at the maximum and minimum applied stress levels, respectively.

It can be concluded from Equations 2 and 3 that, before an accurate fracture analysis or prediction of crack growth rate of a cracked element can be made, the crack size and shape, among other needed parameters, must be known precisely. More important, one should be able to detect small cracks because, as can be determined from Equation 3, most of the fatigue life is exhausted while a crack is small.

The presence of small cracks can have a significant influence on the remaining fatigue lives of structures. In steel highway bridge structures, various types of welded details are used. Most of these details contain discontinuities or imperfections that are created during the fabrication stage. Discontinuities of various sizes and frequencies, depending on the welding process, geometrical configurations of the welded details, and workmanship, are introduced in the welded structures. Previous fatigue studies of the welded components have shown that fatigue cracks were initiated from discontinuities with maximum depths of less than 0.016 in. (0.4 mm) at the toe of welds and from embedded defects, such as gas pockets, with a maximum radius of less than 0.08 in. (2 mm) (*1,3,5,6*). In many structures such as highway bridges, the structural members are normally subjected to cyclic loading, and the fatigue cracks are not visible until over 90 percent of the fatigue lives are expended. Clearly, to have a detection capability at a relatively early life stage that can provide adequate time for the necessary remedial work without compromising the safety of the public and producing traffic disruption is desirable.

Detection of small fatigue cracks by conventional nondestructive evaluation (NDE) techniques, such as visual, dye penetrant, magnetic particles, ultrasonic, and x-ray, is usually unreliable or costly, or both. The difficulty and cost of detection are significant because a majority of the discontinuities reside in regions of complex geometry. Past research studies (*7,8*) have shown that the probability of detection of such small discontinuities is low, even during the NDE of simple geometries and under controlled conditions.

To predict the remaining fatigue life of a component with an existing crack, the initial size of the crack is assumed to be the largest discontinuity that cannot be detected by the conventional NDE methods. Because the size of an undetectable crack or discontinuity can be relatively large, the assumption used here can result in an overly conservative estimate of the fatigue life or an uneconomical design of the component. Therefore, it is desirable to develop and use a more accurate and reliable NDE method capable of detecting

small fatigue cracks and of evaluating the status of a growing crack at various stages of its life.

The capability of acoustic emission (AE) for detection and evaluation of fatigue cracks is examined in two structural steels that are used in construction of highway bridge structures. An experimental laboratory investigation that included an AE study during fatigue testing of a series of full-sized beams was followed by an AE field test of an in-service steel bridge structure. The experimental procedures and results of the study are described herein.

ACOUSTIC EMISSION

AE consists of transient elastic waves that are generated by sudden releases of stored elastic energy from localized sources within a medium, e.g., by growth of a defect. In other words, they are produced by the occurrence of some dynamic processes at a micromechanism level in a material that is approaching a state of equilibrium. Normally, partitioning of the released energy takes place and only a fraction of this energy is converted into AE. These stress waves can be detected at various surface points of a component by highly sensitive transducers. The transducers convert the mechanical surface phenomenon to electrical voltage as a function of time, which may be evaluated to obtain information about the source.

Generation of AE results from large numbers of mechanisms or sources. These mechanisms include moving and piling up of dislocations, phase transformation, twinning, slippage at the grain boundaries, electrical discharges, and initiation and propagation of cracks. On the macromechanism level, these mechanisms generally include only plastic deformation and crack initiation and propagation.

EXPERIMENTAL PROGRAM

Constant cyclic loading was applied to full-sized beam specimens while the AE technique was used for detection and evaluation of fatigue cracks. The specimens were made of ASTM A588 weathering steel and A7 steel that are commonly found in existing steel bridges. The A588 beams were new, welded, plate girders; the A7 specimens were beams with extensive evidence of corrosion. The A7 beams were obtained from an old bridge that had been taken out of service before the beginning of the work. A total of seven A588 and seven A7 steel beams were included in this study. Each specimen was tested over a clear span of 15 ft. The geometrical configuration of the welded specimens and the AE transducer layout are shown in Figures 1 and 2. The A7 specimens had section properties similar to those of an S-type beam (S 15 × 42.9) (*9*). The AE transducer layout for the A7 beams was the same as that used for the A588 specimens (see Figures 1 and 2). The test values for the yield and ultimate strengths for the A588 steel were 455 MPa (66 ksi) and 606 MPa (88 ksi), respectively. Those values for the A7 steel were 227 MPa (33 ksi) and 448 MPa (65 ksi), respectively.

The constant cyclic loading of the specimens was performed by subjecting the beams to a four-point, bending-type load in a loading frame equipped with a 222.5-kn (50-kip) hydraulic load actuator. The specimens were divided into two groups

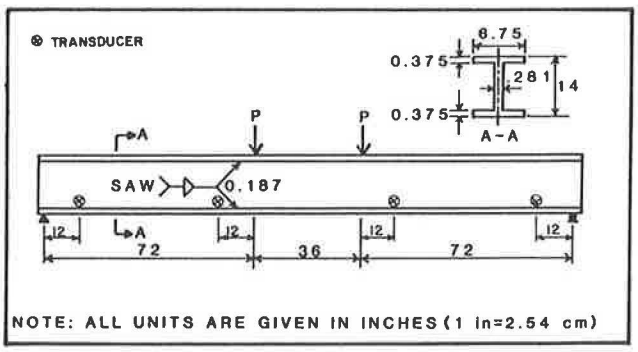

FIGURE 1 Geometrical configuration of welded beam specimens.

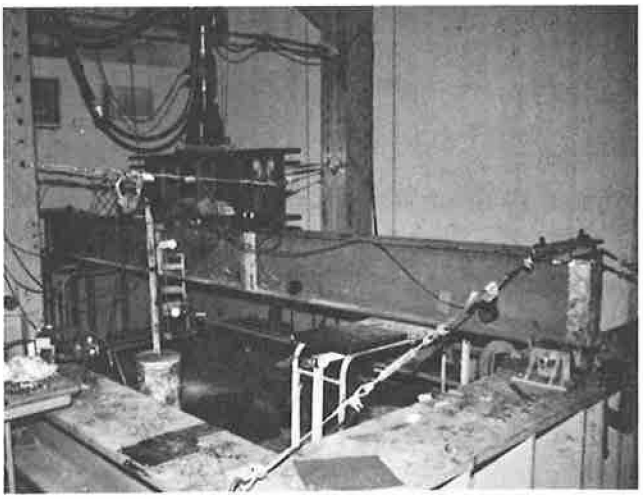

FIGURE 2 Loading frame assembly for testing of beam specimens.

and a different stress range was applied to the specimens in each group. The applied loading was sinusoidal and in a tension-tension fashion with a lower stress limit of 6.89 MPa (1.0 ksi) and a loading frequency of 2.5 Hz (see Tables 1 and 2).

The positions of fatigue crack tips, as indicated by AE, were examined carefully throughout the tests by using a traveling microscope, an ultrasonic unit, and a magnetic contour probe.

At the conclusion of the fatigue experiments, the fracture surfaces of the specimens were examined with a scanning electron microscope to determine the sources of crack initiation and to evaluate the material's microstructure for identification of various regions in the welded beams, namely, weld metal, heat-affected zone, and base metal. AE signals from fatigue cracks, with their tips advancing in these regions, were identified and characterized further at the conclusion of the tests.

A four-channel, acoustic emission testing system was used for this study. Time domain AE measurement was made by using 150-kHz resonant piezoelectric transducers and 100- to 300-kHz band-pass filters. Frequency domain AE data were obtained by using a wide-band filter and a contact piezoelectric transducer with a flat response point that was developed by the National Institute of Standards and Technology. The

TABLE 1 FATIGUE TEST RESULTS FOR A588 WELDED BEAMS

Specimens (1)	σr^a (Ksi) (2)	N_t/1000 (cycles) (3)	Crack Detection % of N_t (4)
1	24	1,649	48
2	24	1,764	54
3	24	2,413	62
4	24	2,429	63
5	30	1,264	52
6	30	1,200	63
7	30	1,240	63

$^a\sigma_{min}$ = 1.0 Ksi.

Note: 1.0 Ksi = 6.89 MPa.

TABLE 2 FATIGUE TEST RESULTS FOR A7 ROLLED BEAMS

Specimens (1)	σr^a (Ksi) (2)	N_t/1000 (cycles) (3)	Crack Detection % of N_t (4)
1	27	1,360	69
2	27	2,532	71
3	27	154	62
4	27	388	56
5	27	359	68
6	27	1,090	58
7	24	226	49

$^a\sigma_{min}$ = 1.0 Ksi

Note: 1.0 Ksi = 6.89 mpa.

total amplification of the AE system was set at 80 db and a threshold level of 30 db was used during the tests. Load values during each cycle were recorded at a time resolution of 10 msec and were correlated to the corresponding AE signals.

An AE study of an in-service bridge was also performed. Signal characteristics from various sources in the bridge, such as traffic and member rubbing, were determined by using the time and frequency domain information.

RESULTS AND DISCUSSION

Laboratory Tests

Test results from the fatigue study of the specimens are presented in Tables 1 and 2. In these tables, σ_r and N_t are the applied stress range and the total fatigue life, respectively. The stress range is computed on the basis of the uncracked, cross-sectional area of each specimen. Fatigue life for each specimen was determined as the total number of load cycles from the beginning of each test to the specimen's failure. The last column of the tables presents the initial AE indication of fatigue crack activity as a percentage of the total fatigue life for each specimen. It is not clear that this initial AE indication of crack activity is from an actual crack initiation stage or from subsequent slow crack growth. However, it is of special interest to be able to detect fatigue crack activity at these early stages. The position for the tip of each fatigue crack, as indicated by AE, was marked and monitored throughout the test and was verified visually and by using the ultrasonic unit, traveling microscope, and magnetic contour probe. In all tests, verification of the indicated fatigue crack positions was successful.

All fatigue cracks in the rolled beams originated at the sites of the corrosion pits that were on the surface of the tension flanges. The large scatter observed in the fatigue lives of the rolled beams is attributed to the random orientation and severity of the corrosion pits that were formed on the beams.

In the welded beams, all fatigue cracks were initiated at discontinuities in the fillet welds at the junction of the tension flange and web. A typical source of fatigue crack initiation in a welded beam specimen is shown in Figure 3.

AE signals from the fatigue crack activities and noise sources were analyzed in both the time and frequency domains. Most mechanical noise sources during the laboratory and field investigations produced AE signals that contained predominant frequency components below 50 kHz. When the frequency components were larger than 50 kHz, the noise-related signal amplitudes were diminished by approximately 20 db or more. An average frequency spectrum for a typical signal related to mechanical noise in a beam specimen is shown in Figure 4. During the field testing of the steel bridge, similar spectra were obtained for signals from sources related to traffic noise (see Figure 5). As a result of this finding, band-pass electronic filters (100 to 300 kHz) were used in the AE system to minimize the signals related to undesirable noise. The upper frequency cut-off value for the filters was determined on the

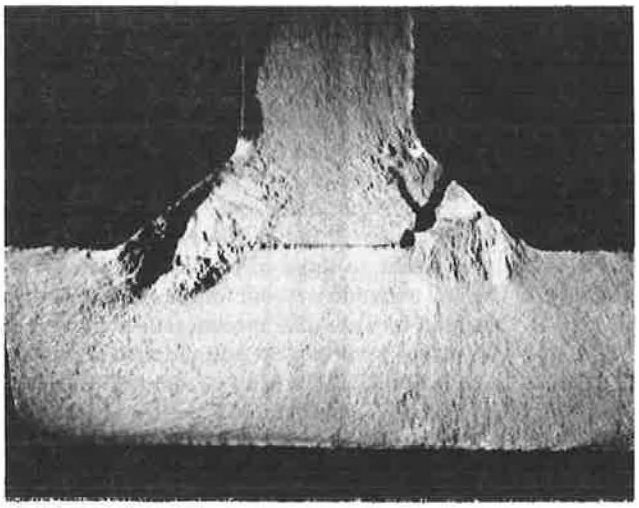

FIGURE 3 A gas pocket in the longitudinal fillet weld of a welded beam.

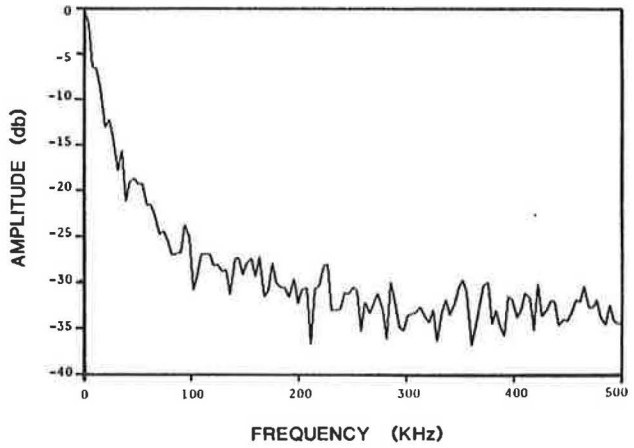

FIGURE 4 Average frequency spectrum for mechanical noise in a beam specimen.

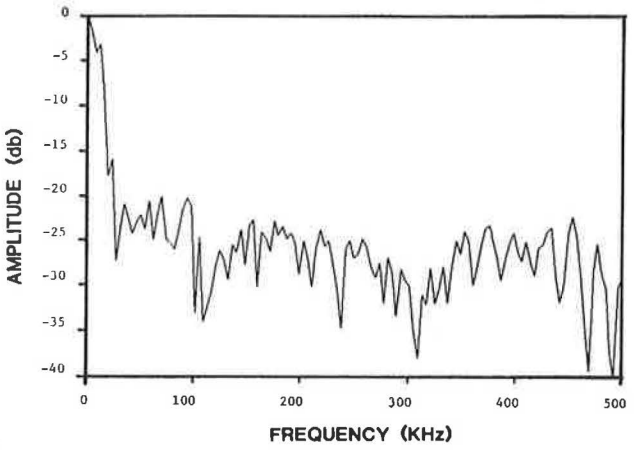

FIGURE 5 Average frequency spectrum for traffic noise in an in-service steel bridge (floor beam).

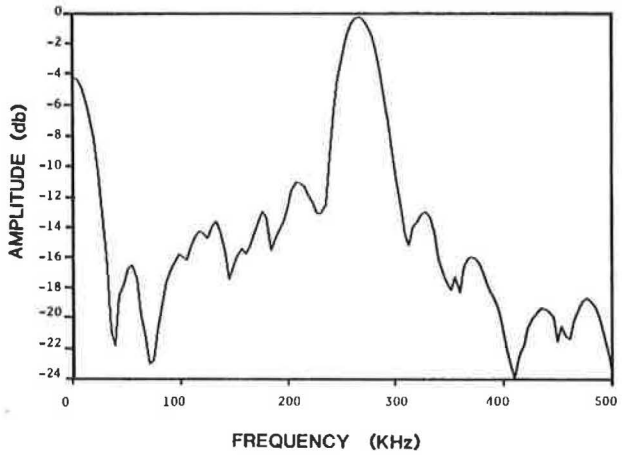

FIGURE 6 Average frequency spectrum for fatigue cracks at 62 percent of life of an A588 welded beam (Specimen 3).

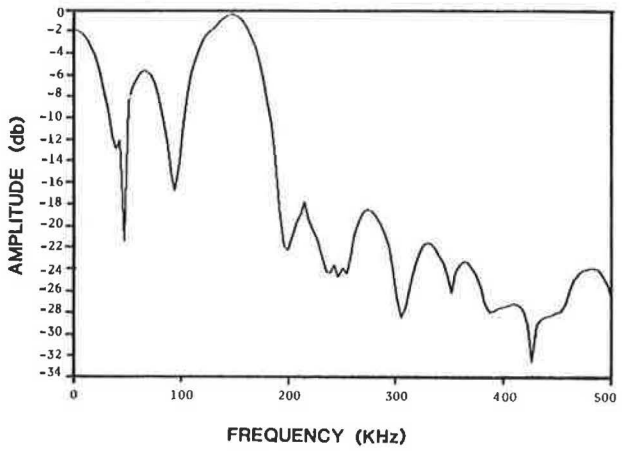

FIGURE 7 Average frequency spectrum for fatigue cracks at 98 percent of life of an A588 welded beam (Specimen 3).

basis of the findings of the frequency analysis of AE signals from the active fatigue cracks in this study.

A significant finding of this work originated in the evaluation of the average frequency spectra for fatigue crack activities at various stages of the life of each specimen. The predominant frequencies in the spectra were higher at early stages of fatigue life and gradually moved towards lower values when the number of load cycles became greater. This observation was consistent for all experiments conducted in this study. Figures 6 and 7 show the average frequency spectra for a growing fatigue crack in one of the welded beams at an early stage (62 percent of total life) and at a late stage (98 percent of life), respectively. Both figures show average frequency values for 10 consecutive crack-related signals. Similar-frequency spectra were obtained for the A7 steel specimens. The change in the average frequency for the A588 steel specimens was from 280 to 152 kHz, and for the A7 steel specimens it was from 253 to 124 kHz. Tables 3 and 4 present the ranges of the average frequency values, listed at various percentages of the life for the A588 and A7 beams, respectively.

A simplified approach was also used to determine the frequency content of the acoustic waves. This approximate frequency analysis uses the time domain data and the following relationship to compute the various equivalent frequency components f:

$$f = \mu \cdot \frac{N}{T} \cdot 10^6 \tag{4}$$

where μ is a proportionality constant, initially taken as unity (1.0) and verified later in this study; and N and T are the total number of signal counts and duration, respectively, measured above a preset threshold level of 30 db. The constant 10^6 is a normalizing factor. Comparison of the frequency information obtained from Equation 4 and from the frequency domain data for the A588 specimens resulted in an average computed value for μ of 1.06, and a standard deviation of 0.03. The computed average value for μ was 1.04 and the standard deviation was 0.09 when the A7 specimens were considered. The earlier assumption of $\mu = 1.0$ may therefore be approximately justified.

The change in the predominant frequency components of the signals from the growing fatigue cracks may be rationalized from the point of view of dynamic fracture mechanics. Correlations have been established between the instantaneous

TABLE 3 RANGE OF FREQUENCY VALUES FOR A588 BEAMS

Specimens (1)	Frequency at Initial Crack Detection[a], KHz (2)	Frequency Just Before Fracture, KHz (3)
1	262	144
2	280	148
3	275	158
4	275	148
5	278	152
6	285	152
7	302	160
AVERAGE	280	152

[a]See Table 1 for percentages of life at the initial crack activity detection by AE

TABLE 4 RANGE OF FREQUENCY VALUES FOR A7 BEAMS

Specimens (1)	Frequency at Initial Crack Detection[a], KHz (2)	Frequency Just Before Fracture, KHz (3)
1	252	123
2	250	120
3	244	118
4	258	126
5	262	126
6	256	133
7	252	122
AVERAGE	253	124

[a]See Table 1 for percentages of life at the initial crack activity detection by AE

stress intensity factor K and the crack velocity V, by using dynamic photoelasticity (*10,11*). It has been shown that the crack velocity in a material suddenly increases from a stationary state to a relatively high value when K reaches a value representing the arrest toughness of the material K_{Ic}. Further increase in K beyond K_{Ic} results in a constant crack velocity subsequent to a small transition zone. Further, the frequency of an AE signal because of a crack growth increment with length sf may be determined from

$$f = \frac{v}{s} \tag{5}$$

With increase in the number of load cycles, during which length s of each crack growth increment becomes larger, and for a constant crack velocity v, it can be seen from Equation 5 that f gradually decreases.

The results from the frequency analysis of the AE signals from the specimens indicate that an effective signal

ination scheme may be used by performing a fast Fourier transformation (FFT) of an AE signal in a bridge member for its identification as a crack- or noise-related signal. Further, from the frequency analysis of a crack-related signal from a bridge member, it will be possible to estimate the remaining fatigue life of the member by comparing the computed peak-frequency component of the signal with the lower and upper frequency values obtained during the laboratory tests.

In the time domain, AE signal parameters, such as signal peak amplitude, counts, duration, rise time, and energy level, were measured. Signals in the laboratory and bridge studies related to mechanical noise showed a wide spread in the acquired time domain data. Signal duration values were on the order of 750 μsec and longer, and the rise time values were approximately 50 μsec and longer. The scatter in the data for the other parameters was large and therefore they were not used in developing a signal discrimination routine. Interference from the signals related to mechanical noise was somewhat minimized by using a front end filter, which incorporated the time domain information on the signal duration and rise time, as described.

In general, all AE signals from fatigue crack propagation in the tested specimens were of relatively low intensity. This was due to the high ductility of the materials used and the resulting low level of energy released at the crack tip for each crack growth increment. Two records of AE signals from a growing fatigue crack in a welded beam specimen at an early stage (54 percent of life) and late stage (98 percent of life) are shown in Figures 8 and 9, respectively. The figures also show the corresponding applied cyclic stress level as a function of time. In Figure 8, the occasional occurrence of low-level, crack-related, burst-type AE signals was produced near the maximum stress level. The continuous-type signals shown in Figures 8 and 9 were related to the plastic deformation associated with crack tip reversal, and the burst-type signals near the lower stress level were related to the hydraulic machine noise and were of no significance. At later loading cycles, the occurrence of the burst-type AE signals, with higher intensity levels, was observed at each cycle of the loading. Figure 9 shows a crack-related AE signal at the maximum stress level

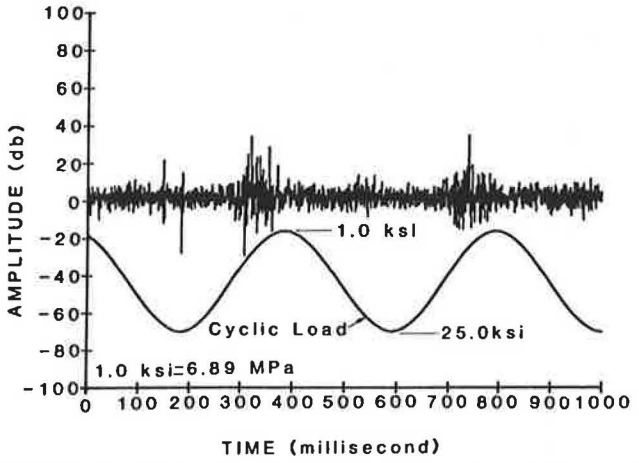

FIGURE 8 AE signals at incipient fatigue cracking in the weld metal of a welded beam specimen at 54 percent of life (Specimen 2).

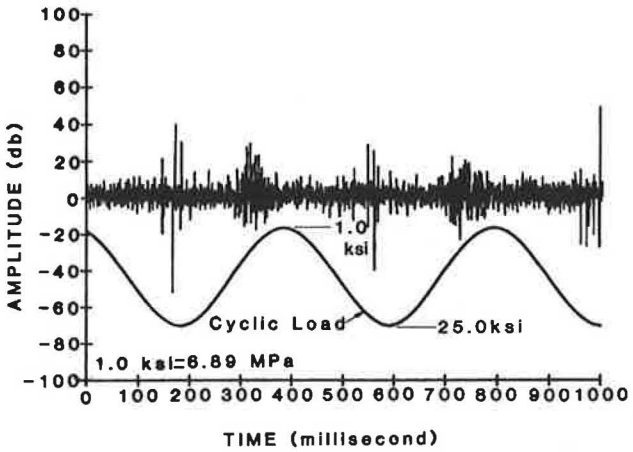

FIGURE 9 AE signals in the weld metal of a welded beam specimen at 98 percent of life (Specimen 2).

for each load cycle at 98 percent of the life of a welded specimen.

In the welded beam specimens, the characteristic features of AE signals were significantly changed as the crack tip, which had initiated in the weld metal, advanced into the heat-affected zone and the base metal. The signal amplitude levels and other AE parameters increased in values during the crack propagation within the weld metal. However, as the crack tip advanced into the heat-affected zone, and subsequently into the base metal, the signal amplitude and other AE parameters showed a decrease in their values. The variation of the signal amplitude (with 95 percent confidence level) with respect to the position of the fatigue crack tip in a welded beam and the rate of crack growth *da/dN* are shown in Figure 10. All crack tip locations during crack growth were verified by using the ultrasonic unit, traveling microscope, and magnetic contour probe. The signal intensity decreased in spite of the fact that the rate of crack growth *da/dN* was increased rapidly. Subsequent microscopic examination of the fracture surfaces demonstrated a combination of flat fractured facets with high reflectivity and some dimples that indicated a mix of brittle and ductile modes of fracture in the weld metal. Study of the fracture surfaces showed that in the heat-affected zone and

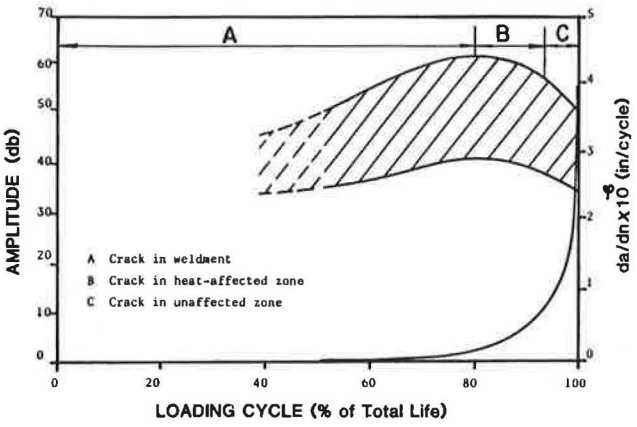

FIGURE 10 Amplitude of AE signals and fatigue crack growth rate at various stages of life of a welded beam (Specimen 2).

the base metal the fracture was closer to a plastic type with numerous dimples, which were observed on the surfaces.This finding is in agreement with the results of the fracture toughness measurement of various welded bridge beams (*12*). The lower level signal intensities from the crack tip movement within the heat-affected zone and the base metal were the result of the void coalescent and plastic deformation in those regions. Lower signal intensity caused by plastic deformation was also observed by others (*13*). Except for final load cycles just before fracture of the A7 rolled beams, the values for the signal amplitude and other AE parameters were consistently increased with increasing number of loading cycles, because there were no changes in the material's microstructure, i.e., because of welding. Signal amplitude and other AE parameters decreased in magnitude for the final cycles of loading because of the presence of a large degree of plasticity at each crack tip. Generally, the signal amplitudes from crack growth in the weld metal were about 33 percent higher when compared to the results from the rolled beams.

Use of the information obtained during this investigation allowed for successful separation of fatigue-related AE signals from undesirable ones, namely, noise-related signals. The information also permitted detection of the incipient fatigue cracking at relatively early stages of the fatigue life (see Tables 1 and 2). For example, fatigue cracks in the welded beams were first detected by AE at stages ranging from 48 to 63 percent of the total fatigue lives of the beams. Locations of growing fatigue cracks were determined by measuring times of arrival of AE signals to two data transducers. The distance between the calculated position of each crack tip and the actual crack site, as determined by analyzing AE signals, was generally less than 2 percent of the distance between the two data transducers.

Field Test

An in-service steel highway bridge was tested for detection of fatigue cracking. The bridge was constructed from ASTM A373 steel, which is similar to the A7 steel used in the laboratory study during this work. A known fatigue problem area in the bridge was at the ends of floor beams where connections to main girders were made. The floor beams were coped at each end at a right angle and without a gradual transition, causing stress concentration (see Figure 11). Several fatigue cracks had been previously identified in the bridge and had been repaired by drilling a hole at each crack tip. An AE test of a segment of the bridge was performed during this study to evaluate the effectiveness of the previous remedial work and to examine other details that had not been identified with fatigue cracking. No fatigue crack activities were observed by AE in the details that had been repaired. A small fatigue crack, approximately 0.3 mm, was detected by AE at the coping of a floor beam at one of the end connections to a main girder. The presence of the crack was also verified by an ultrasonic evaluation of the area. From the frequency analysis of the AE signals emitted from the crack, a peak-frequency component of 255 kHz was determined, which indicated a fatigue crack activity at an early stage. Because cross-sectional dimensions in the bridge members are larger than those in the laboratory specimens, a plain-strain state of stress, which causes a brittle type of fracture, is expected. As a result, AE signals with lower durations, or higher frequencies, are produced. Tests of larger specimens must be performed to verify this effect and to develop the necessary data for use during field evaluation. Results from the time domain analysis of the AE signals from the fatigue crack in the floor beam are presented in Table 5. Because of the scatter in the time domain AE data, the lower and upper limits with 95 percent confidence levels are shown in the table.

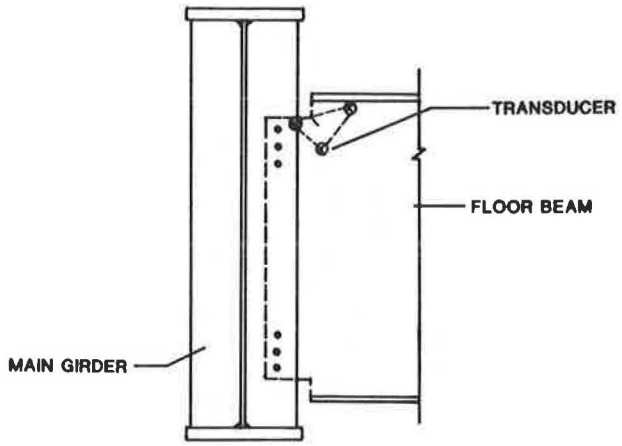

FIGURE 11 A typical detail for connection at a floor beam end and a main girder.

CONCLUSION

Use of AE for early detection of active fatigue cracks in highway bridge structural components was discussed. An experimental study that included test specimens made of ASTM A588 and A7 steels was conducted. AE signals from growing fatigue cracks were analyzed for their time and frequency domain characteristics. AE signals from growing fatigue cracks at different stages of their lives contained distinct characteristic features, which can be used for identification of the sources of emission. Fatigue cracks, in all laboratory specimens, were detected at relatively early stages of fatigue lives of the corresponding specimens.

To detect active fatigue cracks at relatively early stages of the fatigue lives of steel highway bridge members by using AE is possible. Early detection in steel bridges can provide

TABLE 5 RANGE OF CRACK-RELATED AE PARAMETERS IN THE BRIDGE

AE Parameters (1)	Lower Limit (2)	Upper Limit (3)
Amplitude	32 dB	35 dB
Duration	15 μs	55 μs
Rise Time	3 μs	8 μs
Counts	5	25
Energy	3	20

adequate warning and ensure the safety of the traveling public. Additionally, a safe and economical remedial work with minimum disturbance of the traffic can be planned. AE may also permit, under normal traffic loading, the assessment of the behavior of existing bridge elements with known defects. By using AE, it is possible to accurately determine whether an existing crack is active. As a result, costly repairs may only be applied to areas with active fatigue cracking.

REFERENCES

1. J. W. Fisher, K. H. Frank, M. A. Hirt, and B. M. McNamee. *NCHRP Report 102: Effect of Weldments on the Fatigue Strength of Steel Beams*. TRB, National Research Council, Washington, D.C., 1970.
2. M. A. Hirt. *Fatigue Behavior of Rolled and Welded Beams*. Ph.D. dissertation. Lehigh University, Bethlehem, Pa., 1971.
3. J. W. Fisher, P. A. Albrecht, B. T. Yen, D. J. Klingerman, and B. M. McNamee. *NCHRP Report 147: Fatigue Strength of Steel Beams with Welded Stiffeners and Attachments*. TRB, National Research Council, Washington, D.C., 1974.
4. P. C. Paris, M. P. Gomes, and W. E. Anderson. A Rational Analytic Theory of Fatigue. *The Trend in Engineering*, Vol. 13, 1961, pp. 9–14.
5. E. G. Signes, et al. Factors Affecting the Fatigue Strength of Welded High Strength Steels. *British Welding Journal*, Vol. 14, No. 3, 1967.
6. F. Watkinson, et al. The Fatigue Strength of Welded Joints in High Strength Steels and Methods for its Improvement. *Proc., Conference on Fatigue of Welded Structures*, The Welding Institute, Brighton, England, 1970.
7. J. M. Barsom and S. T. Rolfe. *Fracture and Fatigue Control in Structures, Applications of Fracture Mechanics*. Prentice-Hall, Englewood Cliffs, N.J., 1987.
8. W. C. Clark. Some Problem in the Application of Fracture Mechanics. Scientific paper 79-1D3-SRIDS-P1, Westinghouse Research and Development Center, Pittsburgh, Pa., 1979.
9. *Manual of Steel Construction*. 8th ed., American Institute of Steel Construction, Inc., 1986.
10. T. Kobayashi and J. W. Dally. A System of Modified Epoxies for Dynamic Photoelastic Studies of Fracture. *Experimental Mechanics*, Vol. 17, No. 10, 1977, pp. 367–374.
11. T. Kobayashi and J. W. Dally. Dynamic Photoelastic Determination of the a-K Relation for 4340 Alloy Steel. *Crack Arrest Methodology and Applications, ASTM STP 711*. G. T. Hahn and M. F. Kanninen, eds., ASTM, Philadelphia, Pa., 1980, pp. 189–210.
12. J. U. Yung. *Mechanical Testing of Welds*. Report FHWA/RD-83/006. FHWA, U.S. Department of Transportation, 1984.
13. A. A. Pollock. Acoustic Emission: Basic Considerations and Energy Transfer and Some Structural Testing Results. Presented at the Institute of Physics Conference on Acoustic Emission, Imperial College, London, England, 1972.

Publication of this paper sponsored by Committee on Structures Maintenance.